

DESY 03-217
 hep-ph/0401137

INSTANTON-DRIVEN SATURATION AT SMALL X^*

F. SCHREMPF

*Deutsches Elektronen Synchrotron (DESY),
 Notkestrasse 85,
 D-22607 Hamburg, Germany
 E-mail: fridger.schrempp@desy.de*

A. UTERMANN

*Institut für Theoretische Physik der Universität Heidelberg,
 Philosophenweg 16,
 D-69120 Heidelberg, Germany
 E-mail: A.Utermann@thphys.uni-heidelberg.de*

We report on the interesting possibility of instanton-driven gluon saturation in lepton-nucleon scattering at small Bjorken- x . Our results crucially involve non-perturbative information from high-quality lattice simulations. The conspicuous, intrinsic instanton size scale $\langle\rho\rangle \approx 0.5$ fm, as known from the lattice, turns out to determine the saturation scale. A central result is the identification of the “colour glass condensate” with the QCD-sphaleron state.

1. Motivation

1.1. *Saturation in the Parton Picture*

One of the most important observations from HERA is the strong rise of the gluon distribution at small Bjorken- x ¹. On the one hand, this rise is predicted by the DGLAP evolution equations² at high Q^2 and thus supports QCD³. On the other hand, an undamped rise will eventually violate unitarity. The reason for the latter problem is known to be buried in the linear nature of the DGLAP- and the BFKL-equations⁴: For decreasing Bjorken- x , the number of partons in the proton rises, while their effective size $\sim 1/Q$ increases with decreasing Q^2 . At some characteristic scale $Q^2 \approx Q_s^2(x)$, the gluons in the proton start to overlap and so the linear approximation is no longer applicable; non-linear corrections to the linear evolution equations⁵ arise and become significant, potentially taming the

*Presented at the Ringberg Workshop: *New Trends in HERA Physics 2003*, Sep. 28 – Oct. 3, 2003, Ringberg Castle, Rottach-Egern, Germany.

growth of the gluon distribution towards a “saturating” behaviour.

1.2. Instantons and Saturation?

eP -scattering at small Bjorken- x and decreasing Q^2 uncovers a novel regime of QCD, where the coupling α_s is (still) small, but the parton densities are so large that conventional perturbation theory ceases to be applicable. Much interest has recently been generated through association of the saturation phenomenon with a multiparticle quantum state of high occupation numbers, the “Colour Glass Condensate” that correspondingly, can be viewed⁶ as a strong *classical* colour field $\propto 1/\sqrt{\alpha_s}$.

Being extended non-perturbative and topologically non-trivial fluctuations of the gluon field, instantons⁷ (I) are naturally very interesting in the context of saturation, since

- classical *non-perturbative* colour fields are physically appropriate;
- the functional form of the instanton gauge fields is explicitly known and their strength is $A_\mu^{(I)} \propto \frac{1}{\sqrt{\alpha_s}}$ as needed;
- an identification of the “Colour Glass Condensate” with the QCD-sphaleron state appears very suggestive^{8,9} (c.f. below and Sec 3.2).

Two arguments in favour of instanton-driven saturation are particularly worth emphasizing.

We know already from I -perturbation theory that the instanton contribution tends to strongly increase towards the softer regime^{10,11,12}. The mechanism for the decreasing instanton suppression with increasing energy is known since a long time^{13,14}: Feeding increasing energy into the scattering process makes the picture shift from one of tunneling between adjacent vacua ($E \approx 0$) to that of the actual creation of the sphaleron-like, coherent multi-gluon configuration¹⁵ on top of the potential barrier of height^{10,16} $E = m_{\text{sph}} \propto \frac{1}{\alpha_s \rho_{\text{eff}}}$.

A crucial aspect concerns the I -size ρ . On the one hand it is just a collective coordinate to be integrated over in any observable, with the I -size distribution $D(\rho) = dn_I/d^4z d\rho$ as universal weight. On the other hand, according to lattice data, $D(\rho)$ turns out to be *sharply* peaked (Fig. 1 (left)) around $\langle \rho \rangle \approx 0.5$ fm. Hence instantons represent truly non-perturbative gluons that bring in naturally an intrinsic size scale $\langle \rho \rangle$ of hadronic dimension. As we shall see, $\langle \rho \rangle$ actually determines the saturation scale^{21,8,9}.

Presumably, it is also reflected in the conspicuous *geometrization* of soft QCD at high energies^{22,21,8}. For related approaches associating instantons

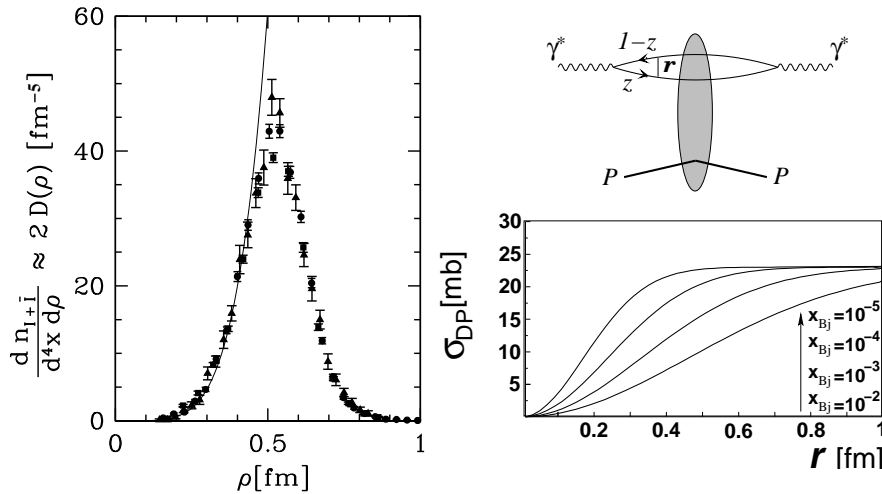


Figure 1. (Left) UKQCD lattice data^{17,18,19} of the $(I+\bar{I})$ -size distribution for quenched QCD ($n_f = 0$). Both the sharply defined I -size scale $\langle \rho \rangle \approx 0.5$ fm and the parameter-free agreement with I -perturbation theory^{18,19} (solid line) for $\rho \lesssim 0.35$ fm are apparent. (Right) $\gamma^* p$ scattering at small x . The photon fluctuates into a $q\bar{q}$ dipole interacting with the proton (top). Generic behaviour of the dipole-proton cross section, as taken from the GBW-model²⁰ (bottom).

with high-energy (diffractive) scattering, see Refs.^{23,24,25,14}. Instantons in the context of small- x saturation have also been studied recently by Shuryak and Zahed²⁶, with conclusions differing in part from those of our preceding work^{22,21,8,9}. Their main emphasis rests on Wilson loop scattering, and lattice information was not used in their approach.

In this paper we shall report about our results on the interesting possibility of instanton-driven saturation at small Bjorken- x . They have been obtained by exploiting crucial non-perturbative information from high-quality lattice simulations^{17,18}.

2. Setting the Stage

The investigation of saturation becomes most transparent in the familiar colour-dipole picture²⁷ (cf. Fig. 1 (top right)), notably if analyzed in the so-called dipole frame²⁸. In this frame, most of the energy is still carried by the hadron, but the virtual photon is sufficiently energetic, to dissociate before scattering into a $q\bar{q}$ -pair (a *colour dipole*), which then scatters off the hadron. Since the latter is Lorentz-contracted, the dipole sees it as a colour source of transverse extent, living (essentially) on the light cone.

This colour field is created by the constituents of the well developed hadron wave function and – in view of its high intensity, i.e. large occupation numbers – can be considered as classical. Its strength near saturation is $\mathcal{O}(1/\sqrt{\alpha_s})$. At high energies, the lifetime of the $q\bar{q}$ -dipole is much larger than the interaction time between this $q\bar{q}$ -pair and the hadron and hence, at small x_{Bj} , this gives rise to the familiar factorized expression of the inclusive photon-proton cross sections,

$$\sigma_{L,T}(x_{\text{Bj}}, Q^2) = \int_0^1 dz \int d^2\mathbf{r} |\Psi_{L,T}(z, r)|^2 \sigma_{\text{DP}}(r, \dots). \quad (1)$$

Here, $|\Psi_{L,T}(z, r)|^2$ denotes the modulus squared of the (light-cone) wave function of the virtual photon, calculable in pQCD, and $\sigma_{\text{DP}}(r, \dots)$ is the $q\bar{q}$ -dipole-nucleon cross section. The variables in Eq. (1) are the transverse ($q\bar{q}$)-size \mathbf{r} and the photon’s longitudinal momentum fraction z carried by the quark. The dipole cross section is expected to include in general the main non-perturbative contributions. For small r , one finds within pQCD^{27,29} that σ_{DP} vanishes with the area πr^2 of the $q\bar{q}$ -dipole. Besides this phenomenon of “colour transparency” for small $r = |\mathbf{r}|$, the dipole cross section is expected to saturate towards a constant, once the $q\bar{q}$ -separation r exceeds a certain saturation scale r_s . While there is no direct proof of the saturation phenomenon, successful models incorporating saturation do exist^{20,30} and describe the data efficiently.

Let us outline more precisely the strategy we shall pursue:

The guiding question is: Can background instantons of size $\sim \langle \rho \rangle$ give rise to a saturating, geometrical form for the dipole cross section,

$$\sigma_{\text{DP}}^{(I)}(r, \dots) \stackrel{r \gtrsim \langle \rho \rangle}{\sim} \pi \langle \rho \rangle^2 \quad (2)$$

We have obtained answers from two alternative approaches^{22,21,8,9}:

- (1) *From I-perturbation theory to saturation:* Here, we start from the large Q^2 regime and appropriate cuts such that I -perturbation theory is strictly valid. The corresponding, known results on I -induced DIS processes³¹ are then transformed into the colour-dipole picture. With the crucial help of lattice results, the $q\bar{q}$ -dipole size r is next carefully increased towards hadronic dimensions. Thanks to the lattice input, IR divergencies are removed and the original cuts are no longer necessary.
- (2) *Wilson-loop scattering in an I-background:* As a second, complementary approach we have considered the semi-classical, non-abelian eikonal approximation. It results in the identification of the

$q\bar{q}$ -dipole with a Wilson loop, scattering in the non-perturbative colour field of the proton. The field $A_\mu^{(I)} \propto \frac{1}{\sqrt{\alpha_s}}$ due to background instantons is studied as a concrete example, leading to analytically calculable results in qualitative agreement with the first approach.

3. From I -Perturbation Theory to Saturation

3.1. The Simplest Process: $\gamma^* + g \xrightarrow{(I)} q_R + \bar{q}_R$

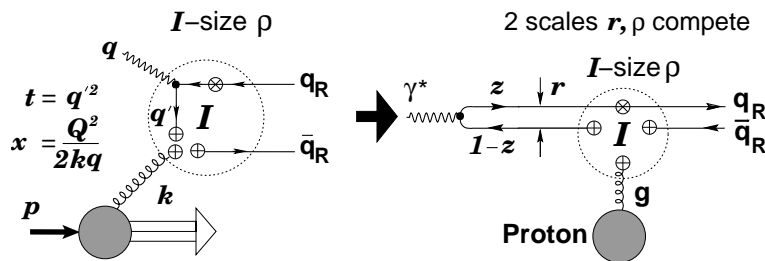


Figure 2. Transcription of the simplest I -induced process into the colour-dipole picture

Let us briefly consider first the simplest I -induced process, $\gamma^* g \Rightarrow q_R \bar{q}_R$, with one flavour and no final-state gluons (Fig. 2 (left)). More details may be found in Ref.⁸. Already this simplest case illustrates transparently that in the presence of a background instanton, the dipole cross section indeed saturates with a saturation scale of the order of the average I -size $\langle \rho \rangle$.

We start by recalling the results for the total $\gamma^* N$ cross section within I -perturbation theory from Ref.³¹,

$$\sigma_{L,T}(x_{Bj}, Q^2) = \int_{x_{Bj}}^1 \frac{dx}{x} \left(\frac{x_{Bj}}{x} \right) G \left(\frac{x_{Bj}}{x}, \mu^2 \right) \int dt \frac{d\hat{\sigma}_{L,T}^{\gamma^* g}(x, t, Q^2)}{dt}; \quad (3)$$

$$\frac{d\hat{\sigma}_L^{\gamma^* g}}{dt} = \frac{\pi^7}{2} \frac{e_q^2}{Q^2} \frac{\alpha_{em}}{\alpha_s} \left[x(1-x)\sqrt{tu} \frac{\mathcal{R}(\sqrt{-t}) - \mathcal{R}(Q)}{t + Q^2} - (t \leftrightarrow u) \right]^2 \quad (4)$$

with a similar expression for $d\hat{\sigma}_T^{\gamma^* g}/dt$. Here, $G(x_{Bj}, \mu^2)$ denotes the gluon density and L, T refers to longitudinal and transverse photons, respectively.

Note that Eqs. (3), (4) involve the “master” integral $\mathcal{R}(Q)$ with dimension of a length,

$$\mathcal{R}(Q) = \int_0^\infty d\rho D(\rho) \rho^5(Q\rho) K_1(Q\rho). \quad (5)$$

In usual I -perturbation theory, the ρ -dependence of the I -size distribution $D(\rho)$ in Eq.(5) is known³² for sufficiently small ρ ,

$$D(\rho) \approx D_{I\text{-pert}}(\rho) \propto \rho^{6-\frac{2}{3}n_f}, \quad (6)$$

the strong power law increase of which, is well known to generically lead to (unphysical) IR-divergencies from large-size instantons. However, in DIS for sufficiently large virtualities \mathcal{Q} , the crucial factor $(\mathcal{Q}\rho) K_1(\mathcal{Q}\rho) \sim e^{-\mathcal{Q}\rho}$ in Eq.(5) exponentially suppresses large size instantons and I -perturbation theory holds, as shown first in Ref.³¹.

The effective size $\mathcal{R}(\mathcal{Q})$ in Eq.(5) correspondingly plays a central rôle in the context of a continuation of our I -perturbative results to smaller \mathcal{Q} . Here, crucial lattice information enters. We recall that the I -size distribution $D_{\text{lattice}}(\rho)$, as *measured* on the lattice^{17,18,19}, is strongly peaked around an average I -size $\langle \rho \rangle \approx 0.5$ fm (cf. Fig. 1 (left)), while being in excellent, parameter-free agreement^{18,19} with I -perturbation theory for $\rho \lesssim 0.35$ fm (cf. Fig. 1 (left)).

Our general strategy is thus to generally identify $D(\rho) = D_{\text{lattice}}(\rho)$ in Eq.(5), whence

$$\mathcal{R}(0) = \int_0^\infty d\rho D_{\text{lattice}}(\rho) \rho^5 \approx 0.3 \text{ fm} \quad (7)$$

becomes finite and a \mathcal{Q}^2 cut is no longer necessary.

By means of an appropriate change of variables and a subsequent $2d$ -Fourier transformation, Eqs. (3), (4) may indeed be cast⁸ into a colour-dipole form (1), e.g. (with $\hat{Q} = \sqrt{z(1-z)} Q$)

$$\begin{aligned} (|\Psi_L|^2 \sigma_{\text{DP}})^{(I)} &\approx |\Psi_L^{\text{pQCD}}(z, r)|^2 \frac{1}{\alpha_s} x_{\text{Bj}} G(x_{\text{Bj}}, \mu^2) \frac{\pi^8}{12} \\ &\times \left\{ \int_0^\infty d\rho D(\rho) \rho^5 \left(\frac{-\frac{d}{dr^2} \left(2r^2 \frac{K_1(\hat{Q}\sqrt{r^2+\rho^2/z})}{\hat{Q}\sqrt{r^2+\rho^2/z}} \right)}{K_0(\hat{Q}r)} - (z \leftrightarrow 1-z) \right) \right\}^2. \end{aligned} \quad (8)$$

The strong peaking of $D_{\text{lattice}}(\rho)$ around $\rho \approx \langle \rho \rangle$, implies

$$(|\Psi_{L,T}|^2 \sigma_{\text{DP}})^{(I)} \Rightarrow \begin{cases} \mathcal{O}(1) \text{ but exponentially small;} & r \rightarrow 0, \\ |\Psi_{L,T}^{\text{pQCD}}|^2 \frac{1}{\alpha_s} x_{\text{Bj}} G(x_{\text{Bj}}, \mu^2) \frac{\pi^8}{12} \mathcal{R}(0)^2; \frac{r}{\langle \rho \rangle} \gtrsim 1. \end{cases} \quad (9)$$

Hence, the association of the intrinsic instanton scale $\langle \rho \rangle$ with the saturation scale r_s becomes apparent from Eqs. (8), (9): $\sigma_{\text{DP}}^{(I)}(r, \dots)$ rises strongly as function of r around $r_s \approx \langle \rho \rangle$, and indeed *saturates* for

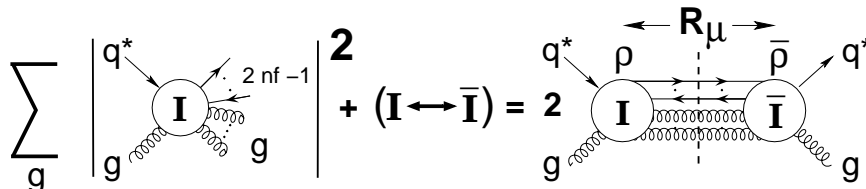


Figure 3. Optical theorem for the I -induced q^*g - subprocess. The incoming, virtual q^* originates from photon dissociation, $\gamma \rightarrow \bar{q} + q^*$.

$r/\langle\rho\rangle > 1$ towards a *constant geometrical limit*, proportional to the area $\pi \mathcal{R}(0)^2 = \pi (\int_0^\infty d\rho D_{\text{lattice}}(\rho) \rho^5)^2$, subtended by the instanton. Since $\mathcal{R}(0)$ would be divergent within I -perturbation theory, the information about $D(\rho)$ from the lattice (Fig. 1 (left)) is crucial for the finiteness of the result.

3.2. The Realistic Process: $\gamma^* + g \xrightarrow{(I)} n_f (q_R + \bar{q}_R) + \text{gluons}$

On the one hand, the inclusion of an arbitrary number of final-state gluons and $n_f > 1$ light flavours causes a significant complication. On the other hand, it is due to the inclusion of final-state gluons that the identification of the QCD-sphaleron state with the colour glass condensate has emerged^{8,9}, with the qualitative “saturation” features of the preceding subsection remaining unchanged. In view of the limited space, let us therefore focus our main attention in this section to the emerging sphaleron interpretation of the colour glass condensate.

Most of the I -dynamics resides in I -induced q^*g -subprocesses like

$$q_L^*(q') + g(p) \xrightarrow{(I)} n_f q_R + (n_f - 1) \bar{q}_R + \text{gluons}, \quad (10)$$

with an incoming off-mass-shell quark q^* originating from photon dissociation, $\gamma \rightarrow \bar{q} + q^*$. The important kinematical variables are the total I -subprocess energy $E = \sqrt{(q' + p)^2}$ and the quark virtuality $Q'^2 = -q'^2$.

It is most convenient to account for the arbitrarily many final-state gluons by means of the so-called “ $I\bar{I}$ -valley method”³³. It allows to achieve via the optical theorem (cf. Fig. 3) an elegant summation over the final-state gluons in form of an exponentiation, with the effect of the gluons residing entirely in the $I\bar{I}$ -valley interaction $-1 \leq \Omega_{\text{valley}}^{I\bar{I}}(\frac{R^2}{\rho\bar{\rho}} + \frac{\rho}{\bar{\rho}} + \frac{\bar{\rho}}{\rho}; U) \leq 0$, between I 's and \bar{I} 's. The new collective coordinate R_μ denotes the $I\bar{I}$ -distance 4-vector (cf. Fig. 3), while the matrix U characterizes the $I\bar{I}$ relative colour orientation. Most importantly, the functional form of $\Omega_{\text{valley}}^{I\bar{I}}$ is

analytically known^{34,35} and the limit of I -perturbation theory is attained for $\sqrt{R^2} \gg \sqrt{\rho\bar{\rho}}$.

The strategy we shall apply, is identical to the one for the “simplest process” in the previous Sec. 3.1: Starting point is the general form of the I -induced γ^*N cross section, this time obtained by means of the $I\bar{I}$ -valley method¹¹. By exploiting the optical theorem (cf. Fig. 3), the total q^*g -cross section is most efficiently evaluated from the imaginary part of the forward elastic amplitude induced by the $I\bar{I}$ -valley background. The next step is again a variable and $2d$ -Fourier transformation into the colour-dipole picture like before.

The dipole cross section $\tilde{\sigma}_{\text{DP}}^{(I),\text{gluons}}(\mathbf{l}^2, x_{\text{Bj}}, \dots)$ before the final $2d$ -Fourier transformation^a $\mathbf{l} \leftrightarrow \mathbf{r}$ to the dipole size \mathbf{r} , arises simply as an energy integral over the I -induced total q^*g cross section from Ref.¹¹,

$$\tilde{\sigma}_{\text{DP}}^{(I),\text{gluons}} \approx \frac{x_{\text{Bj}}}{2} G(x_{\text{Bj}}, \mu^2) \int_0^{E_{\text{max}}} \frac{dE}{E} \left[\frac{E^4}{(E^2 + Q'^2) Q'^2} \sigma_{q^*g}^{(I)}(E, \mathbf{l}^2, \dots) \right], \quad (11)$$

involving in turn integrations over the $I\bar{I}$ -collective coordinates $\rho, \bar{\rho}, U$ and the $I\bar{I}$ -distance R_μ .

In the softer regime of interest for saturation, we again substitute $D(\rho) = D_{\text{lattice}}(\rho)$, which enforces $\rho \approx \bar{\rho} \approx \langle \rho \rangle$ in the respective $\rho, \bar{\rho}$ -integrals, while the integral over the $I\bar{I}$ -distance R is dominated by a *saddle point*,

$$\frac{R}{\langle \rho \rangle} \approx \text{function} \left(\frac{E}{m_{\text{sph}}} \right); \quad m_{\text{sph}} \approx \frac{3\pi}{4} \frac{1}{\alpha_s \langle \rho \rangle} = \mathcal{O}(\text{few GeV}). \quad (12)$$

At this point, the mass m_{sph} of the QCD-sphaleron^{10,16}, i.e the barrier height separating neighboring topologically inequivalent vacua, enters as the scale for the I -subprocess energy E . The saddle-point dominance of the R -integration implies a one-to-one relation,

$$\frac{R}{\langle \rho \rangle} \Leftrightarrow \frac{E}{m_{\text{sph}}}; \quad \text{with } R = \langle \rho \rangle \Leftrightarrow E \approx m_{\text{sph}}. \quad (13)$$

Our careful continuation to the saturation regime now involves in addition to the I -size distribution $D_{\text{lattice}}(\rho)$, crucial lattice information about the second basic building block of the I -calculus, the $I\bar{I}$ -interaction $\Omega^{I\bar{I}}$. The relevant lattice observable is the distribution of the $I\bar{I}$ -distance^{18,8}

^aThe 2-dimensional vector \mathbf{l} denotes the transverse momentum of the quark with four-momentum q'

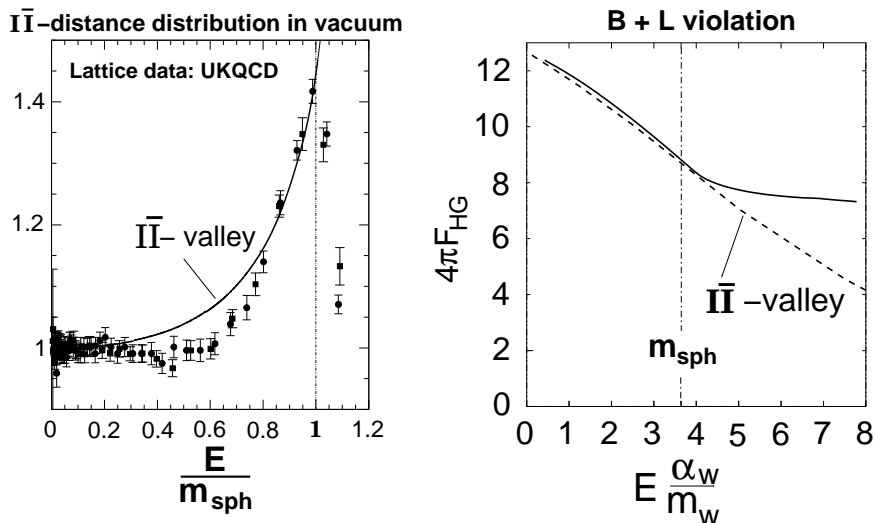


Figure 4. (Left) UKQCD lattice data^{17,18} of the (normalized) $I\bar{I}$ -distance distribution and the corresponding $I\bar{I}$ -valley prediction⁸ displayed versus energy in units of the QCD sphaleron mass m_{sph} . The lattice data provide the first direct evidence that the $I\bar{I}$ -valley approach is adequate right up to $E \approx m_{\text{sph}}$, where the dominant contribution to the scattering process arises. Beyond this point a marked disagreement rapidly develops. (Right) The same trend for electroweak $B + L$ -violation is apparent from a completely independent semiclassical, numerical simulation of the suppression exponent for two-particle collisions ('Holy Grail' function) $F_{\text{HG}}(E)$ ^{36,37}.

$R = \sqrt{R_\mu^2}$, essentially providing information on $\left\langle \exp\left[-\frac{4\pi}{\alpha_s} \Omega^{I\bar{I}}\right] \right\rangle_{U,\rho,\bar{\rho}}$ in Euclidean space. Due to the crucial saddle-point relation (12), (13), we may replace the original variable $R/\langle\rho\rangle$ by E/m_{sph} . A comparison of the respective $I\bar{I}$ -valley predictions with the UKQCD lattice data^{17,18,8} versus E/m_{sph} is displayed in Fig. 4 (left). It reveals the important result that the $I\bar{I}$ -valley approximation is quite reliable up to $E \approx m_{\text{sph}}$. Beyond this point a marked disagreement rapidly develops: While the lattice data show a *sharp peak* at $E \approx m_{\text{sph}}$, the valley prediction continues to rise indefinitely for $E \gtrsim m_{\text{sph}}$! It is most remarkable that an extensive recent and completely independent semiclassical numerical simulation³⁶ shows precisely the same trend for electroweak $B + L$ -violation, as displayed in Fig. 4 (right). Also here, there is an amazing agreement with the valley approximation³⁷ up to the electroweak sphaleron mass, and a rapid disagreement developing beyond. It is again at hand to identify $\Omega^{I\bar{I}} = \Omega_{\text{lattice}}^{I\bar{I}}$ for $E \gtrsim m_{\text{sph}}$. Then, on account of Eq. (11), the integral over the I -subprocess energy spectrum in

the dipole cross section appears to be dominated by the sphaleron configuration at $E \approx m_{\text{sph}}$. The feature of saturation analogously to the “simplest process” in Sec. 3.1 then implies the announced identification of the colour glass condensate with the QCD-sphaleron state.

4. Wilson-Loop Scattering in an I -Background

Let us next turn to our second approach within the colour-dipole picture, which is still in progress^{9,38}. It is complementary to our previous strategy of extending the known results of I -perturbation theory towards the saturation regime by means of non-perturbative lattice information. $q\bar{q}$ -dipole scattering will be described as the scattering of Wilson loops.

We work within the semiclassical, non-abelian eikonal approximation that is appropriate for the scattering of partons at high energies ($s \gg -t$ or small x_{Bj}) from a soft colour field A_μ ³⁹. The basic approximation is that the soft interaction of the partons with the colour field does not change their direction appreciably, such that they just pick up a non-abelian phase factor during the scattering. Each phase factor is given by a path-ordered integral calculated along the classical path of the respective parton,

$$W(\mathbf{x}) = \text{P exp} \left\{ -i g_s \int_{-\infty}^{+\infty} d\lambda q^\mu A_\mu(\lambda q + x_\perp) \right\}, \text{ with } x_\perp \cdot q = 0. \quad (14)$$

This so-called Wilson line, depends on the 2-dimensional vector \mathbf{x} describing the distance to the proton-photon plane. Correspondingly, $q\bar{q}$ -dipoles lead to colourless, gauge invariant Wilson loops:

$$\mathcal{W}(\mathbf{r}, \mathbf{b}; A_\mu) = \frac{1}{N_c} \text{tr} [W(\mathbf{b} + \mathbf{r}/2) W^\dagger(\mathbf{b} - \mathbf{r}/2)]. \quad (15)$$

The Wilson loop (15) depends on the transverse size \mathbf{r} of the colour dipole and the transverse distance \mathbf{b} between dipole and colour field A_μ . It is a basic object in the framework of the colour glass condensate language, where the proton is viewed as a source of the classical field A_μ . Averaging over possible field configurations ($\langle \dots \rangle_{A_\mu}$) and integrating over the impact parameter \mathbf{b} leads to the total dipole cross section (e.g.^{40,6}),

$$\sigma_{\text{DP}}(r, \dots) = 2 \int d^2\mathbf{b} \langle 1 - \mathcal{W}(\mathbf{r}, \mathbf{b}; A_\mu) \rangle_{A_\mu}. \quad (16)$$

In general, the meaning of the colour glass condensate in the context of the dipole cross section (16) (cf. also Ref.⁴¹) is that of an effective theory, leading to non-linear evolution equations^{40,42} for the respective scattering amplitude.

As a first concrete testing ground for the impact of instantons within this framework, let us identify the classical field A_μ in the dipole cross section (16) with the known instanton field $A_\mu^{(I)}$. The functional integration $\langle \dots \rangle_{A_\mu}$ over the field configurations A_μ is then to be understood as an integration over the I-collective coordinates, i.e.

$$A_\mu(x) \rightarrow A_\mu^{(I)}(x, \rho, x_0); \quad \langle \dots \rangle_{A_\mu} \rightarrow \mathcal{D}A_\mu^{(I)} \rightarrow d^4x_0 d\rho D_{\text{lattice}}(\rho). \quad (17)$$

In a first step, one has to calculate the Wilson loop in the I -background, which can be performed analytically. Subsequently, one has to integrate over the collective coordinates. Finally, we get a dipole cross section depending on the dipole size r and the size $\langle \rho \rangle$ of the instanton in the vacuum,

$$\sigma_{\text{DP}}^{(I)}(r, \dots) \propto \langle \rho \rangle^2 f\left(\frac{r}{\langle \rho \rangle}\right). \quad (18)$$

Like in our first approach (Sec. 3), this dipole cross section turns out to saturate towards a constant limit proportional to $\langle \rho \rangle^2$ for $r \gtrsim \langle \rho \rangle$.

For a more realistic estimate, it is important to notice that one has to take an $I\bar{I}$ -configuration (like the valley field³⁸) in the total cross section (16). For an estimate of the elastic part of the dipole cross section, one can take the single I -gauge field and square the resulting dipole scattering-amplitude. This elastic contribution $\sigma_{\text{DP}}^{(I)}(r)/\sigma_{\text{DP}}^{(I)}(\infty)$, normalized to one for $r \rightarrow \infty$, is displayed in Fig. 5 (left) as function of $r/\langle \rho \rangle$. The importance of $\langle \rho \rangle$ in the approach to saturation becomes again apparent. In Fig. 5 (right), the corresponding impact parameter profile for $r = \langle \rho \rangle, \infty$ is displayed. This simplest estimate of the dipole cross section in an I -background can certainly not describe the proton in an adequate way, notably due to the lack of non-trivial proton kinematics. Hence it is not surprising that the resulting dipole cross section and hence the saturation scale comes out x_{Bj} -independent in this case. Nevertheless, this calculation illustrates once more the close connection between an 'extended' classical colour background field of size $\langle \rho \rangle$ and the saturation scale. Taking the instanton solution as an initial condition for the BK-equations^{40,42}, one could generate the proper x_{Bj} -dependence via the implied evolution.

In order to model the proton more realistically, we have also worked out³⁸ a generalization to dipole-dipole scattering in an I -background. The formalism used is analogous to Ref.⁴³ within the stochastic vacuum approach⁴⁴. Like in Ref.⁴³, we started with the calculation of the loop-loop contributions to the dipole-dipole scattering-amplitude, that are dominant in the large- N_c limit. In this case, the trace in Eq. (15) is taken separately

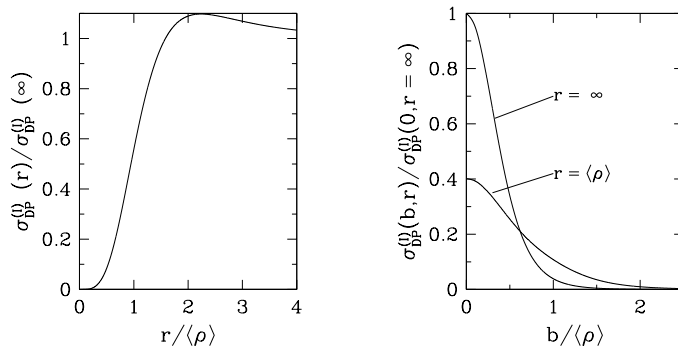


Figure 5. (Left) The elastic contribution to the I-induced dipole cross section (Right) The corresponding impact parameter profile.

for both dipoles. This leads to consistent results and we observe again a saturation of the resulting dipole cross section. In Refs.^{24,25,26} it was pointed out, however, that the dominant contribution in the high-energy limit comes from contribution with a colour exchange between the dipoles. The impact of this contribution for the dipole cross section is presently under investigation³⁸.

Acknowledgments

We are grateful to Andreas Ringwald for a careful reading of the manuscript.

References

1. C. Adloff *et al.* [H1 Collaboration], *Eur. Phys. J.* **C21**, 33 (2001);
S. Chekanov *et al.* [ZEUS Collaboration], *Eur. Phys. J.* **C21**, 443 (2001).
2. V.N. Gribov and L.N. Lipatov, *Sov. J. Nucl. Phys.* **15**, 438 (1972);
L.N. Lipatov, *Sov. J. Nucl. Phys.* **20**, 94 (1975);
G. Altarelli and G. Parisi, *Nucl. Phys.* **B126**, 298 (1977);
Y.L. Dokshitzer, *Sov. Phys. JETP* **46**, 641 (1977).
3. A. De Rujula *et al.*, *Phys. Rev.* **D10**, 1649 (1974).
4. L.N. Lipatov, *Sov. J. Nucl. Phys.* **23**, 338 (1976);
V.S. Fadin, E.A. Kuraev and L.N. Lipatov, *Phys. Lett.* **B60**, 50 (1975),
Sov. Phys. JETP **44**, 443 (1976), *Sov. Phys. JETP* **45**, 199 (1977);
I.I. Balitsky and L.N. Lipatov, *Sov. J. Nucl. Phys.* **28**, 822 (1978).
5. L.V. Gribov, E.M. Levin and M.G. Ryskin, *Nucl. Phys.* **B188**, 555 (1981);
L.V. Gribov, E.M. Levin and M.G. Ryskin, *Phys. Rept.* **100**, 1 (1983).

6. E. Iancu, A. Leonidov and L. D. McLerran, *Nucl. Phys.* **A692**, 583 (2001); E. Ferreira *et al.*, *Nucl. Phys.* **A703**, 489 (2002).
7. A. Belavin *et al.*, *Phys. Lett.* **B59**, 85 (1975).
8. F. Schrempp and A. Utermann, *Phys. Lett.* **B543**, 197 (2002).
9. F. Schrempp and A. Utermann, *Proc. Strong and Electroweak Matter 2002*, Heidelberg, Oct. 2002, ed. M.G. Schmidt, p. 477 [arXiv:hep-ph/0301177].
10. A. Ringwald and F. Schrempp, *Proc. Quarks '94*, ed D.Yu. Grigoriev *et al.* (Singapore: World Scientific) p 170, [arXiv:hep-ph/9411217].
11. A. Ringwald and F. Schrempp, *Phys. Lett.* **B438**, 217 (1998).
12. A. Ringwald and F. Schrempp, *Comput. Phys. Commun.* **132**, 267 (2000).
13. H. Aoyama and H. Goldberg, *Phys. Lett.* **B188**, 506 (1987); A. Ringwald, *Nucl. Phys.* **B330**, 1 (1990); O. Espinosa, *Nucl. Phys.* **B343**, 310 (1990).
14. D.M. Ostrovsky *et al.*, *Phys. Rev.* **D66**, 036004 (2002).
15. F. R. Klinkhamer and N. S. Manton, *Phys. Rev.* **D30**, 2212 (1984).
16. D. Diakonov and V. Petrov, *Phys. Rev.* **D50**, 266 (1994).
17. D.A. Smith and M.J. Teper (UKQCD), *Phys. Rev.* **D58**, 014505 (1998).
18. A. Ringwald and F. Schrempp, *Phys. Lett.* **B459**, 249 (1999).
19. A. Ringwald and F. Schrempp, *Phys. Lett.* **B503**, 331 (2001).
20. K. Golec-Biernat and M. Wüsthoff, *Phys. Rev.* **D59**, 014017 (1999); *Phys. Rev.* **D60**, 114023 (1999).
21. F. Schrempp and A. Utermann, *Acta Phys. Polon.* **B33**, 3633 (2002).
22. F. Schrempp, *J. Phys.* **G28**, 915 (2002).
23. D.E. Kharzeev, Y.V. Kovchegov and E. Levin, *Nucl. Phys.* **A690**, 621 (2001).
24. E. Shuryak and I. Zahed, *Phys. Rev.* **D62**, 085014 (2000).
25. M. A. Nowak, E. V. Shuryak and I. Zahed, *Phys. Rev.* **D64**, 034008 (2001).
26. E. V. Shuryak and I. Zahed, arXiv:hep-ph/0307103.
27. N. Nikolaev and B.G. Zakharov, *Z. Phys.* **C49**, 607 (1990); *Z. Phys.* **C53**, 331 (1992); A.H. Mueller, *Nucl. Phys.* **B415**, 373 (1994).
28. A.H. Mueller, *Parton Saturation - An Overview*, hep-ph/0111244, in *QCD Perspectives on Hot and Dense Matter*, NATO Science Series, Kluwer, 2002.
29. F. E. Low, *Phys. Rev.* **D12**, 163 (1975); L. Frankfurt, G.A. Miller and M. Strikman, *Phys. Lett.* **B304**, 1 (1993).
30. J. Bartels *et al.*, *Phys. Rev.* **D66**, 014001 (2002).
31. S. Moch, A. Ringwald and F. Schrempp, *Nucl. Phys.* **B507**, 134 (1997).
32. G. 't Hooft, *Phys. Rev.* **D14**, 3432 (1976); *Phys. Rev.* **D18**, 2199 (1978) (Erratum).
33. A. Yung, *Nucl. Phys.* **B297**, 47 (1988).
34. V.V. Khoze and A. Ringwald, *Phys. Lett.* **B259**, 106 (1991).
35. J. Verbaarschot, *Nucl. Phys.* **B362**, 33 (1991).
36. F. Bezrukov, D. Levkov, C. Rebbi, V. Rubakov and P. Tinyakov, *Phys. Rev.* **D68**, 036005 (2003)
37. A. Ringwald, *Phys. Lett.* **B555**, 227 (2003); arXiv:hep-ph/0302112.
38. F. Schrempp and A. Utermann, in preparation.
39. O. Nachtmann, *Annals Phys.* **209**, 436 (1991); J.C. Collins and R.K. Ellis, *Nucl. Phys.* **B360**, 3 (1991).
40. I.I. Balitsky, *Phys. Rev. Lett.* **81**, 2024 (1998), *Phys. Rev.* **D60**, 014020

- (1999).
41. W. Buchmüller and A. Hebecker, *Nucl. Phys.* **B476**, 203 (1996).
 42. Y.V. Kovchegov, *Phys. Rev.* **D60**, 034008 (1999).
 43. A. I. Shoshi, F. D. Steffen and H. J. Pirner, *Nucl. Phys.* **A709**, 131 (2002).
 44. A. Krämer and H. G. Dosch, *Phys. Lett.* **B252**, 669 (1990).